Journal of ELECTRONIC MATERIALS, Vol. 46, No. 2, 2017
DOI: 10.1007/s11664-016-5005-4

Dielectric Relaxation Behavior and AC Electrical Conductivity Study of 2-(1,2-Dihydro-7-Methyl-2-Oxoquinoline-5-yl) Malononitrile (DMOQMN)

M.M. EL-NAHASS,[1] E.F.M. EL-ZAIDIA,[1,2] A.A.A. DARWISH,[2,3,4] and G.F. SALEM[1]

1.—Department of Physics, Faculty of Education, Ain Shams University, Roxy, Cairo 11757, Egypt. 2.—Department of Physics, Faculty of Science, University of Tabuk, Tabuk, Saudi Arabia. 3.—Department of Physics, Faculty of Education at Al-Mahweet, Sana'a University, Al-Mahweet, Yemen. 4.—e-mail: aaadarwish@gmail.com

Dielectric relaxation and alternative current conductivity of a new organic compound 2-(1,2-dihydro-7-methyl-2-oxoquinoline-5-yl) malononitrile (DMOQMN) have been investigated. X-ray diffraction (XRD) at room temperature reveals that DMOQMN samples have a polycrystalline structure of the triclinic system. The analysis of the dielectric constant and dielectric loss index suggested the dominant polarization is performed and the Maxwell–Wagner–Sillar type polarization is dominating at low frequency and high temperature. These results have been confirmed by the XRD and dielectric modulus. The estimated relaxation time and the activation energy are 9×10^{-13} s and 0.43 eV, respectively. Our results indicated that the conduction mechanism of DMOQMN is controlled by the correlation barrier hopping (CBH) model.

Key words: Organic compounds, x-ray diffraction, dielectric properties, electrical conductivity

INTRODUCTION

Organic semiconductors have received great attention consistent with their advantages of potential low-cost, flexibility and wide-spread fabrication.[1,2] Organic semiconductors are used in a wide range of optoelectronic and electronic devices, such as field-effect transistors (FETs),[3] organic light-emitting diodes (OLEDs),[4] photovoltaic cells[5,6] and photodetectors.[7]

The screening of new organic semiconductors with certain inserted properties of the electronic devices could be a major area of research. Quinoline is one of the organic families, which is a class of heterocyclic compounds with many pharmaceutical applications.[8–11] It is used as a treatment for cancer and biological activity.[12,13] The quinoline derivatives and complexes are important in vital technological applications such as OLEDs, energy conversion devices and electron transport material.[14] 2-(1,2-dihydro-7-methyl-2-oxoquinoline-5-yl) malononitrile (DMOQMN) is one of the quinoline derivatives and its molecular structure is shown in Scheme 1.

The dielectric relaxation spectroscopy (DRS) gives evidence about the orientation and translation adjustment of the mobile charges present in the dielectric medium.[15–18] This method is sensitive to the molecular fluctuation of dipoles inside the structure of semiconductor material. These fluctuations are related to the molecular mobility of groups, dipoles or whole segments of the material. The contributions of dielectric polarization components such as electronic, ionic and orientational polarization are responsible for the variation of the dielectric constant values.[17,18] Moreover, at low frequency and high temperature, the material becomes electrically conductive and shows an increase in the dielectric constant, ε, as a result of the interfacial polarization and electrode polarization. In polycrystalline semiconductors, the

(Received March 21, 2016; accepted September 28, 2016; published online November 3, 2016)

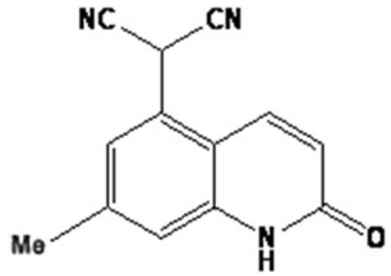

Scheme 1. Molecular structure of 2-(1,2-dihydro-7-methyl-2-oxo-quinoline-5-yl) malononitrile (DMOQMN) compound.

interfacial polarization is due to the trapping of free charge carriers at the boundaries, which exist between crystalline phases.[19] Despite the technological applications of this material in OLED technology[20] and as emitting materials,[21] the literature survey shows a lack of study of dielectric relaxation and alternating current (AC) conductivity for DMOQMN materials. Because cyanide (CN), carbonyl (C=O) and NH groups have a strong dipole moment, relaxation processes of DMOQMN can be examined. Therefore, in this work we have investigated the structure, dielectric relaxation and the AC conductivity of DMOQMN for the first time. Moreover, we have investigated the structure of DMOQMN by using Fourier transform infrared (FTIR) and x-ray techniques.

EXPERIMENTAL TECHNIQUES

The DMOQMN was prepared by direct reaction between 5-chloro-7-methylquin-2-(1H)-one and malononitrile in a molar ratio of 1:1 in the presence of sodium acetate in boiling DMF. The details of DMOQMN synthesis were described previously.[22] The powder of DMOQMN was ground in a mortar to get fine particles. The bulk sample in the form of round pellets (diameter 12 mm; thickness 2.83 mm) was obtained by compressing the DMOQMN powder under a pressure of 2×10^8 Pa. Two gold (Au) electrodes were made on both sides of the pellet using thermal evaporation (Edwards 306A) under a pressure of about 10^{-4} Pa and deposition rate of 2.5 Å/s.

FTIR spectra, in the spectral range 4000 cm^{-1}–400 cm^{-1}, were used to study the molecular structure of DMOQMN using an ATI Mattson IR spectrophotometer. The structural characteristics of DMOQMN were investigated by x-ray diffraction (XRD) patterns. A Philips x-ray diffractometer (model X' pert) operated at 40 kV and 25 mA was used in the measurements utilizing monochromatic CuK_α radiation. The diffraction patterns were recorded naturally with a checking speed of 2° per minute.

The AC conductivity and dielectric measurements were completed utilizing a programmable automatic RLC bridge (Hioki type 3532 Hitester). For the specimen under study, the capacitance, C, the impedance, Z, and the phase angle, ϕ, were

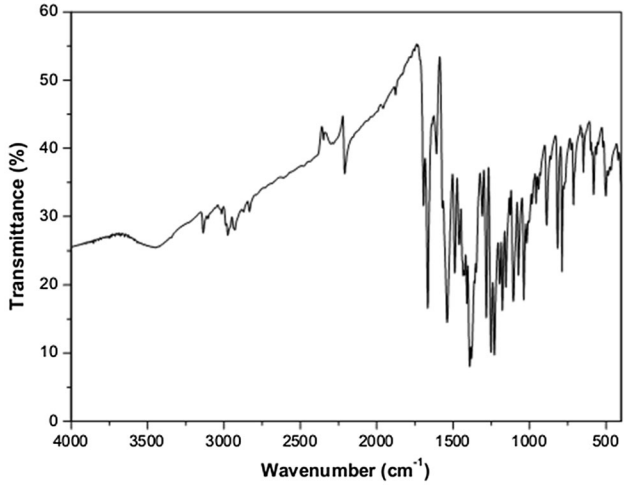

Fig. 1. Fourier transforms infrared (FTIR) spectra for powder DMOQMN.

measured. The dielectric constant, ε', and the dielectric loss, ε'', were recorded in the frequency ranges of 42 Hz–5 MHz and temperature range 303–413 K. The ε' and ε'' were calculated from the equations:

$$\varepsilon' = dC/\varepsilon_o S \quad (1)$$

and

$$\varepsilon'' = \varepsilon' \tan\delta \quad (2)$$

where d is the thickness of the sample, ε_o is the permittivity of free space, S is the surface area of the electrode of the sample holder and $\delta = 90 - \phi$. The total conductivity, σ, was calculated from the following equation: $\sigma = d/ZS$. The temperature of the sample was recorded by using a NiCr–NiAl thermocouple with an accuracy of ±1 K.

RESULTS AND DISCUSSION

Molecular and Crystalline Structure of DMOQMN

FTIR spectroscopy has been utilized to investigate the molecular structure of DMOQMN as shown in Fig. 1. The peak, which is located at 3135 cm^{-1}, is attributed to N–H vibrations. The vibration of aromatic C–H stretching is observed at 3000 cm^{-1} while the band appearing in the region 1072.5–1282.86 cm^{-1} is ascribed to the presence of the C–H in-plane bending vibration and C–H. The out-of-plane bending vibration appears at 712.22 cm^{-1}. The band appearing at 1666.44 cm^{-1} is associated with C=O stretching vibration and the band at 2209.33 is due to C=N vibrations. The asymmetric C–H stretching vibration in CH_3 appears at 2928.69 cm^{-1}.

The XRD pattern of DMOQMN in powder form is shown in Fig. 2. It is clear that many diffraction peaks with different intensities are observed,

showing a polycrystalline structure. Using the CRYSFIRE computer program[23] the system and the lattice constant of DMOQMN sample have been computed. The analysis posted a triclinic structure with lattice parameters a = 10.984 Å, b = 11.045 Å, c = 18.888 Å, α = 101.66°, β = 57.64° and γ = 64.19° and with space group P–1. Moreover, the CHECK-CELL program[24] was used for indexing the Miller indices, which have been calculated and are presented in Fig. 2 for all diffraction peaks of the investigated sample. The obtained values of Miller's indices, hkl, are also shown in Fig. 2.

Dielectric Spectra of DMOQMN

The frequency-temperature dependence of ε' of DMOQMN at some constant temperatures is shown in Fig. 3a. It is clear that the values of ε' decrease gradually with an increase in the frequency and attain almost a constant value at higher values of the field frequency. Also, ε' increases with the increase in temperature. In general, the polarization of the investigated sample is due to electronic, dipolar and space charge polarization. Since the structure of DMOQMN is polycrystalline, the electronic polarization is the most important and contributes to the total polarization process. The decrease in ε' with the increase in the frequency can be attributed as follows: the polarization process of the polar material is due to the contribution of multi-components such as deformational polarization (ionic and electronic) and relaxation polarization (orientation and space charge). As the frequency increases the dipoles due to deformation, polarization will not be able to rotate in the direction of the applied field. With further increasing of the frequency, these dipoles will not be able to completely follow the electric field and polarization is stopped. So, ε' decreased and approached a constant value at higher values of frequency. Consequently, the total polarization, in this case, is mainly due to the space charge polarization. The increase in ε' with the increase in temperature at low frequency indicates that the polarization process of DMOQMN is dipolar in nature.[19] So, the polarization of the dipolar groups (CN, C=O, and NH) plays an important role throughout this process. Obviously, at higher temperatures, these dipoles tend to orient more with the field direction as the thermal agitation facilitates rotation of the dipoles.

The frequency-temperature dependence of ε'' of DMOQMN at some constant temperature exhibits similar behavior and it is depicted in Fig. 3b. The higher values of ε'' at low frequency can be assigned to the crystal structure of DMOQMN, which is polycrystalline with a triclinic crystal system. Thus, the free charge can be gathered at the interphases between these crystal phases near the electrode. This impact can be attributed to the charge trapping of the interface between the polycrystalline phases.[25] So, the Maxwell–Wagner–Sillars (MWS) is predominant as a type of polarization.

The electrical response of polar material like DMOQMN can be analyzed by a complex modulus formalism. An electric modulus formalism is an advantageous gadget to dissect and explain the dynamical parts of the electrical transport phenomena. The major feature of M^* formalism is that the electrode or the interfacial polarization impact can be curbed.[26,27] Usually, in polar material, which is characterized by a conductive component,

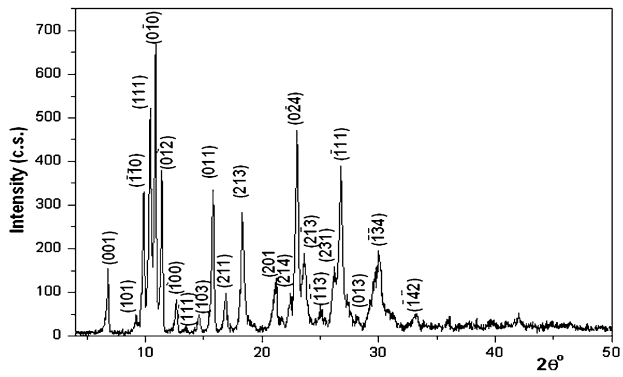

Fig. 2. XRD pattern of DMOQMN in the powder form.

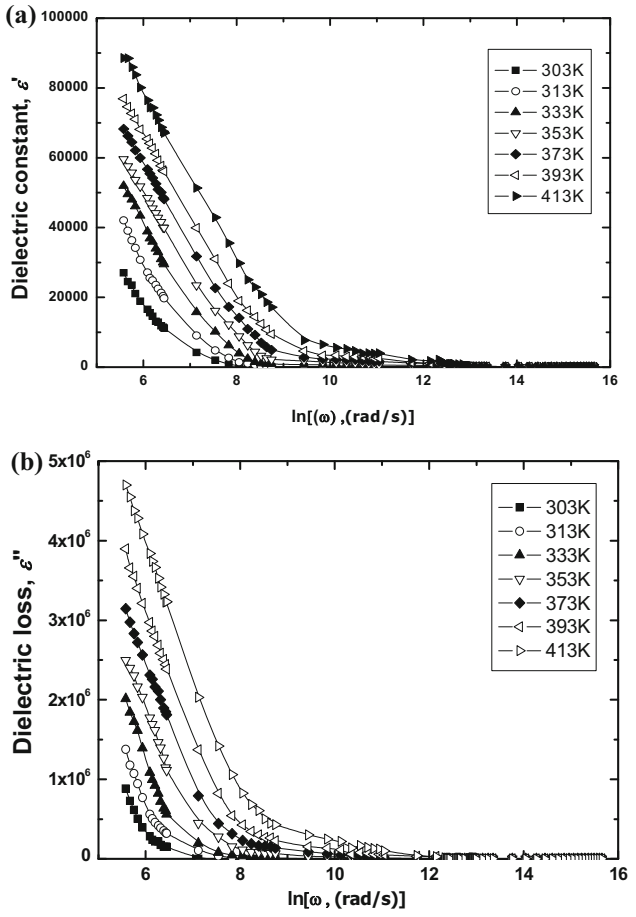

Fig. 3. Frequency dependence of (a) dielectric constant (ε') and (b) dielectric loss (ε'') of DMOQMN at different temperatures.

interfacial polarization is obscured by the conductivity and dielectric permittivity which can take very high values at low frequency and at high temperature. So, to overcome this difficulty, M^* formalism has been used to analyze the electrical conductivity of the polar material.

The complex dielectric modulus $M^*(\omega)$ formulated by[28]:

$$M^*(\omega) = \frac{1}{\varepsilon^*(\omega)} = M' + iM'' \tag{3}$$

$$M' = \frac{\varepsilon'}{\varepsilon'^2 + \varepsilon''^2} \text{ and } M'' = \frac{\varepsilon''}{\varepsilon'^2 + \varepsilon''^2} \tag{4}$$

where M' and M'' are the real and imaginary parts of the dielectric modulus, respectively.

Figure 4a displays the frequency dependence of M' for DMOQMN at some constant temperatures. It is evident that for each temperature, M' reaches a constant value at a higher frequency above 1 MHz. However, M' approaches zero at a lower frequency (400 Hz). This confirms the presence of an appreciable electrode and ionic polarization in the temperature range of study. Therefore, it can suggest that the nature of the crystal structure of DMOQMN, which is polycrystalline, leads to constructing interfaces between the crystalline phases. These interfaces give rise to interfacial polarization or MWS polarization.[29] This phenomenon appears in the heterogeneous structure due to the accumulation of charges at the interfaces and formation space charges close to the electrode. Interfacial polarization results in the permittivity mode and at a high value of ε', decreases rapidly with the increase in the field frequency. For this study, the electric modulus and the relaxation behavior can be attributed to the MWS effect.

Figure 4b shows the frequency dependence of M'' for DMOQMN at some fixed temperatures. A relaxation peak was observed for DMOQMN sample. This pattern provides wider information about the charge transport such as the conduction mechanism, conduction relaxation, and ion dynamics as a function of frequency and temperature.[25] M'' has small values at the low-frequency region, revealing the case of polaron hopping, where the charge carriers are moved over a long distance. Furthermore, M'' has a maximum peak at each temperature, for which a relaxation mechanism is applicable. By increasing the frequency above the peak, the carriers seem to be confined to a potential well, thus becoming mobile over a short distance.[28] As the temperature is increased, the motion of the charge carriers turns out to be faster, leading to a decreased relaxation time, with a subsequent shift of the peak value of M'' toward higher frequencies. This behavior proposes that the relaxation is thermally activated, and charge carrier hopping is occurring.[30]

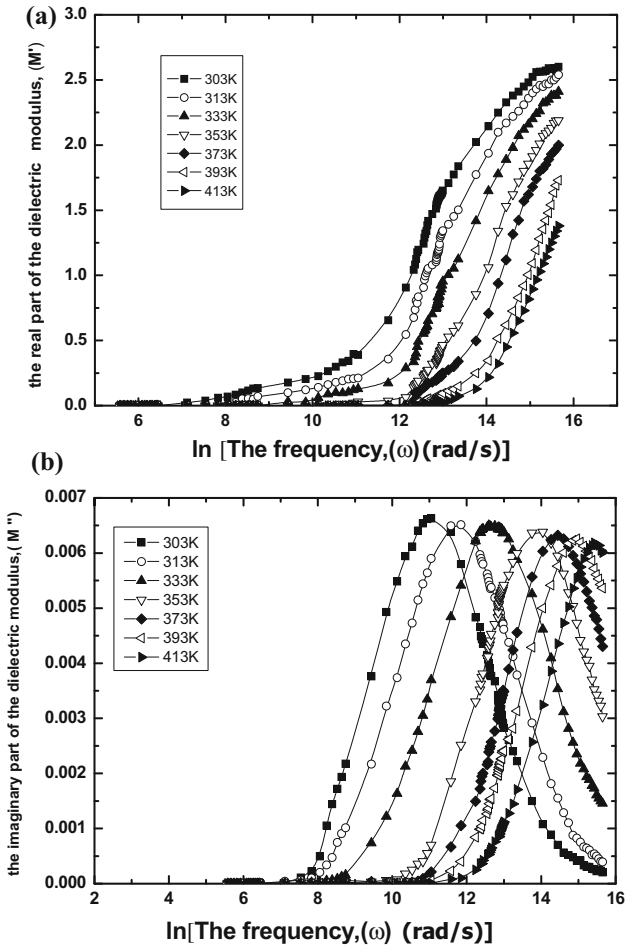

Fig. 4. Frequency dependence of (a) the real part of the dielectric modulus, (M') and (b) the imaginary part of the dielectric modulus, (M'') of DMOQMN at different temperatures.

The conductivity relaxation frequency, ω_m, conforming to M''_{max}, yields the most plausible conductivity relaxation time (τ_m) and it was obtained from the condition $\omega_m\tau_m = 1$. The temperature dependence of τ_m is obtained from M'' spectra shown in Fig. 5. It noted that τ_m exhibits an activated behavior obeying the Arrhenius law[31]:

$$\tau_m = \tau_o \exp(\Delta E_R/k_B T) \tag{5}$$

where τ_o is the relaxation time at infinite temperature, ΔE_R is activation energy and k_B is the Boltzmann constant. The obtained values of τ_o and ΔE_R are calculated from the intercept and slope of the linear fit which equal 9.2×10^{-13} s and 0.43 eV, respectively. The activation energy has a lower value than those reported for some organic compounds.[30]

M'' curves can be reduced to a master curve with ω_m and M''_{max}. Figure 6 illustrates the master curve for DMOQMN samples at some constant temperatures. It is clear that the shape exhibits asymmetric

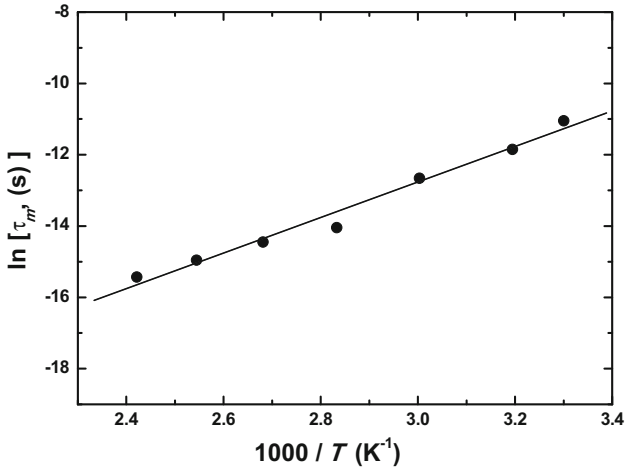

Fig. 5. Temperature dependence of the frequency of the maximum imaginary part of the dielectric modulus, (M''), $\omega_{M''}$, for DMOQMN.

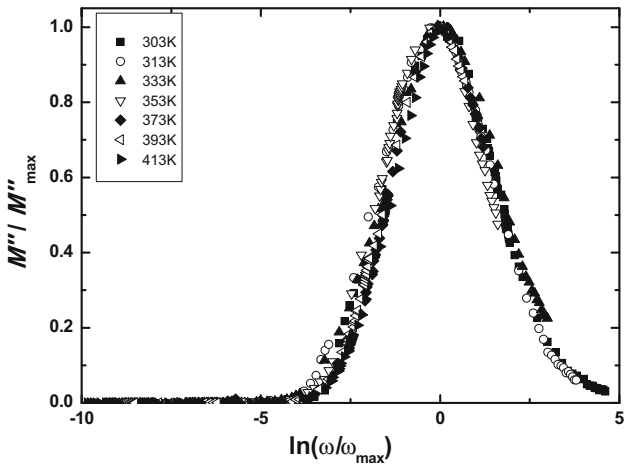

Fig. 6. The normalized plots of M''/M''_{max} versus ln(ω/ω_{max}) for DMOQMN.

behavior and is broader than that of Debye relaxation.[29] This behavior can be described by a non-Debye type of relaxation time governed by[29]

$$\phi(t) = \exp(-t/\tau)^{\beta}, \quad 0 < \beta > 1 \tag{6}$$

where $\phi(t)$ is the time evolution of the electric field in the sample and β is the Kohlrausch exponent. A nonexponential type relaxation governed by Eq. 6 suggested that the ion migration can be taking place via hopping accompanied by a consequential time-dependent mobility of other charge carriers of the same type in the vicinity. This will cause an additional relaxation of the applied electric field.

AC Conductivity of DMOQMN

AC conductivity is an important factor which gives information about the transport phenomenon in materials. It is a good method for determining the

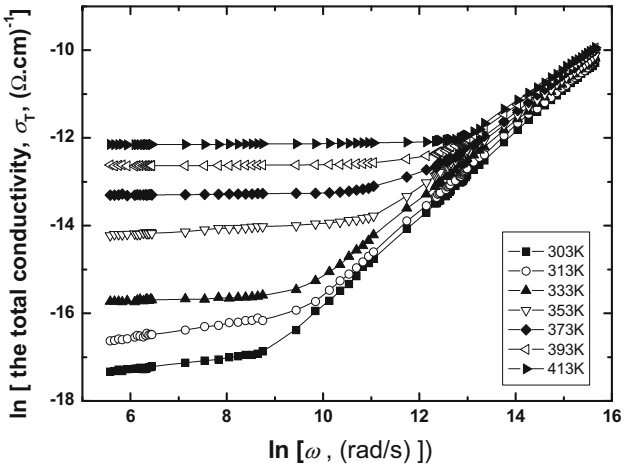

Fig. 7. Variation of the total conductivity, $\sigma_{AC}(\omega)$, with lnω at different temperatures for DMOQMN.

hopping dynamics of the charge carrier. Figure 7 shows the total conductivity, $\sigma(\omega)$, as a function of frequency at different temperatures for a DMOQMN sample. It is clear that the $\sigma(\omega)$ spectra show weak frequency dependence at low frequencies, and then it increases rapidly at higher frequencies. Similar behavior has been observed in many organic materials.[32–43]

The dependence on the frequency of the applied field on the conductivity (σ) can be described by the Jonscher equation[44]:

$$\sigma(\omega) = \sigma_{DC} + \sigma_{AC}(\omega) = \sigma_{DC}(\omega) + A\omega^{s} \tag{7}$$

where σ_{DC} and $\sigma_{AC}(\omega)$ correspond to the DC and AC conductivity, respectively, A is a pre-factor that depends on temperature and composition, ω is the angular frequency and s is the power exponent factor that can take the value range from $0 < s < 1$.[45] The exponent s is very important, which determines the dominant type of conduction mechanisms.[46] The values of the frequency exponent, s, is calculated from the slope of the linear lines of ln σ_{AC} versus lnω and is illustrated in Fig. 8 as a function of temperature. It is observed that the value of s decreases with the increase in temperature and approaches 0.741 at 413 K where the correlated barrier hopping model (CBH)[47] is the most suitable mechanism to describe the AC conductivity of DMOQMN in the study range of temperature. This behavior is in agreement with other organic materials.[32–43]

In a CBH model, the electrical conductivity σ_{AC} due to bipolaron hopping to a first approximation is given by[47]:

$$\sigma_{AC} = \frac{\pi^2 N^2 \varepsilon}{24}\left(\frac{8e^2}{\varepsilon W_M}\right)^6 \frac{\omega^s}{\tau_o^{1-s}} \tag{8}$$

where W_M the maximum barrier height at an infinite inter-site[48] and is given by:

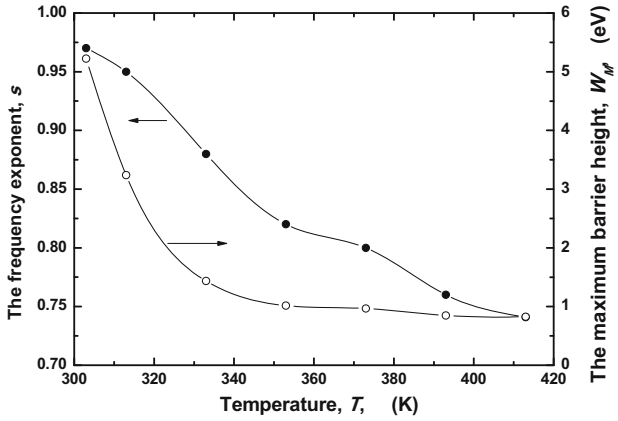

Fig. 8. Temperature dependence of the frequency exponent, (s) and the maximum barrier height, (W_M) for DMOQMN.

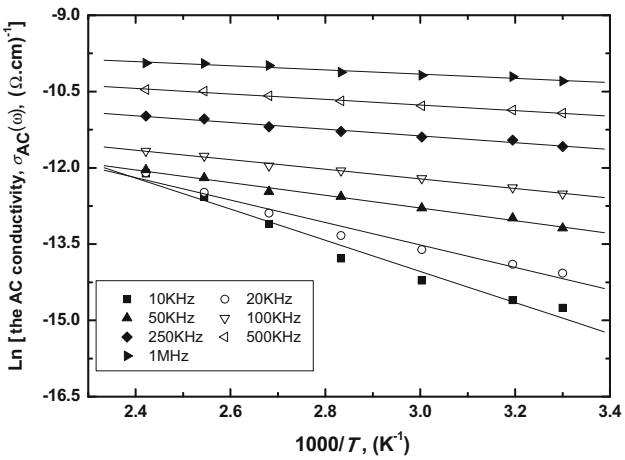

Fig. 9. The variation of $\ln \sigma_{AC}(\omega)$ with 1000/T at different frequencies for DMOQMN.

$$s = 1 - \frac{6k_B T}{W_M} \tag{9}$$

The values of W_M as a function of temperature are shown in Fig. 8. It is observed that W_M decreases with increase in temperature. This leads to the decrease of the exponent s with the increase in temperature.

The temperature dependence of AC conductivity at different frequencies is shown in Fig. 9. It is observed that DMOQMN has a semiconductor behavior in the full range of temperature, where $\ln \sigma_{AC}$ changed linearly with the reciprocal of the absolute temperature. At a higher temperature, $\ln \sigma_{AC}$ has high values; this may be attributed to an increase in the number of charges, which makes hopping increase. The increase in conductivity with the increase in temperature is due to the increase in the thermally activated electron drift velocity of charge carriers according to the hopping conduction

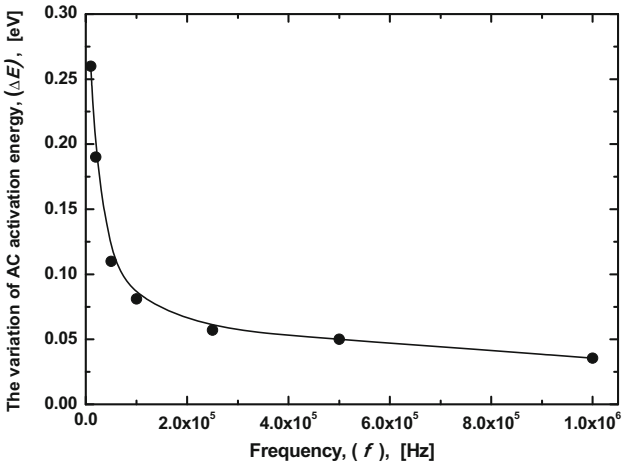

Fig. 10. The variation of AC activation energy, ΔE_{AC} with frequency for DMOQMN.

mechanism. The activation energy calculated from the modified Arrhenius equation of σ_{AC} is given by:

$$\sigma_{AC} = \sigma_o(-\Delta E_{AC}/k_B T) \tag{10}$$

where σ_o is a pre-exponential constant, and ΔE_{AC} is the activation energy of AC conduction.

Figure 10 shows the relation between ΔE_{AC} and the field frequency. It is seen that ΔE_{AC} decreases with the increase in the frequency. This behavior confirms that the conduction mechanism of AC conductivity is controlled by hopping type conduction.[48]

CONCLUSION

The FTIR spectra, XRD, dielectric properties, dielectric modulus and AC conductivity of novel DMOQMN have been investigated. XRD shows that DMOQMN is a triclinic polycrystalline structure. At low frequency and higher temperature, the outcome results of the frequency dependence of ε', ε'', M' and M'' revealed that the interfacial or MWS is the most probable type of polarization. Finally, both electric modulus and AC conductivity indicate that the conduction mechanism of DMOQMN is controlled by CBH type conduction.

ACKNOWLEDGEMENT

The authors are grateful to Prof. T. A. Hanafy, chairman of the Department of Physics, University of Tabuk, Saudi Arabia, for his help and enlightening discussion throughout this work.

REFERENCES

1. M. Arivazhagana and J.S. Kumar, *Spectrochim. Acta Part A* 82, 228 (2011).
2. T.K. Lu and Y.S. Ocak, *Microelectron. Eng.* 88, 151 (2011).
3. Z. Bao, A.J. Lovinger, and A. Dodabalapur, *Appl. Phys. Lett.* 69, 3066 (1996).
4. M. Ishii and Y. Taga, *Appl. Phys. Lett.* 803, 430 (2002).
5. M.M. El-Nahass, K.F. Abd El-Rahman, A.A.M. Farag, and A.A.A. Darwish, *Org. Electron.* 6, 129 (2005).

6. M.M. El-Nahass, H.M. Zeyada, K.F. Abd-El-Rahman, A.A.M. Farag, and A.A.A. Darwish, *Sol. Energy Mater. Sol. Cells* 91, 1120 (2007).
7. P. Peumans, V. Bulovic, and S.R. Forrest, *Appl. Phys. Lett.* 76, 3855 (2000).
8. E. Malle, W. Stadibauer, G. Ostermann, B. Hofmann, H.J. Leis, and G.M. Kostner, *Eur. J. Med. Chem.* 25, 137 (1990).
9. I.V. Ukrainets, S.V. Solobodzyan, V.I. Krivobok, P.A. Bezygly, V.L. Triskach, A.V. Turov, S.V. Gladchenko, and G.V. Obolentseva, *Farm Zh (Kiev)* 2, 78 (1991).
10. I.V. Ukrainets, S.V. Solobodzyan, V.I. Krivobok, P.A. Bezygly, V.L. Triskach, A.V. Turov, S.V. Gladchenko, and G.V. Obolentseva, *Chem. Abstr.* 115, 49362 (1991).
11. E.A. Mohamed, *J. Chem. Soc. Pak.* 13, 166 (1991).
12. V.K. Manohar, M.K. Geeta, C.-H. Lin, and Ch-M Sun, *Curr. Med. Chem.* 13, 2795 (2006).
13. S. Marcaccino, R. Pepino, M. Cruz Pozo, S. Basurto, M. Garia-valverde, and T. Torroba, *Tetrahedron Lett.* 45, 3999 (2004).
14. N.A. El-Ghamaz, M.A. Diab, A.A. El-Bindary, A.Z. El-Sonbati, and S.G. Nozha, *Spectrochim. Acta Part A* 143, 200 (2015).
15. B. Barış, *Phys. E* 54, 171 (2013).
16. V. Laxminarasimha Rao, T. Shekharam, T. Mohan Kumar, and M. Nagabhushanam, *Mater. Chem. Phys.* 159, 83 (2015).
17. Ş. Karataş and Z. Kara, *Microelectron. Reliab.* 51, 2205 (2011).
18. G. Yellaiah, T. Shekharam, K. Hadasa, and M. Nagabhushanam, *J. Alloys Compd.* 609, 192 (2014).
19. S. Mahrous and T.A. Hanfy, *Curr. Appl. Phys.* 4, 461 (2004).
20. M. Rajeswaran, T.N. Blanton, ChW Tang, W.C. Lenhart, S.C. Switalski, D.J. Giesen, B.J. Antalek, T.D. Pawlik, D.Y. Kondakov, N. Zumbulyadis, and R.H. Young, *Polyhedron* 28, 835 (2009).
21. J.-H. Pan, Y.-M. Chou, H.-L. Chiu, B-Ch Wang, and J. Tamkang, *J. Sci. Eng.* 8, 175 (2005).
22. M.M. Ismail, *J. Serb. Chem. Soc.* 71, 721 (2006).
23. R. Shirley, *The CRYSFIRE System for Automatic Powder Indexing: User's Manual* (Guildford, England: The Lattice Press, 2000).
24. J. Laugier and B. Bochu, *LMGP-Suite of Programs for the Interpretation of X-ray Experiments, ENSP/Laboratoire des Matériaux et du Génie Physique, BP 46, 38042* (France: Saint-Martind'Héres, 2000).
25. A. Hassen, T.A. Hanfy, S. El-Sayed, and A. Himanshu, *J. Appl. Phys.* 110, 114119 (2011).
26. R.P. Pawar, *Ceram. Int.* 40, 10423 (2014).
27. S. Mahrous, T.A. Hanfy, and M.S. Sobhy, *Curr. Appl. Phys.* 7, 629 (2007).
28. A.A.A. Darwish, M.M. El-Nahass, and A.E. Bekheet, *J. Alloys Compd.* 586, 142 (2014).
29. T.A. Hanfy, *J. Appl. Phys.* 112, 034102 (2012).
30. A. Karmakar and A. Ghosh, *Curr. Appl. Phys.* 12, 539 (2012).
31. S.K. Rout, A. Hussian, J.S. Lee, I.W. Kim, and S.I. Woo, *J. Alloys Compd.* 11, 477 (2009).
32. A.A.A. Darwish, A.M. Hassanien, T.A. Hanafy, and M.M. El-Nahass, *Synth. Met.* 199, 339 (2015).
33. A.A. Attia, H.S. Soliman, M.M. Saadeldin, and K. Sawaby, *Synth. Met.* 205, 139 (2015).
34. M.M. El-Nahass and H.A.M. Ali, *Solid State Commun.* 152, 1084 (2012).
35. M.M. El-Nahass, A.A. Atta, M.A. Kamel, and S.Y. Huthaily, *Vacuum* 91, 15 (2013).
36. M.M. El-Nahass, A.A. Atta, E.F.M. El-Zaidia, A.A.M. Farag, and A.H. Ammar, *Mater. Chem. Phys.* 143, 490 (2014).
37. E.M. El-Menyawy, H.M. Zeyada, and M.M. El-Nahass, *Solid State Sci.* 12, 2182 (2010).
38. E.M. El-Menyawy, I.T. Zedan, A.M. Mansour, and H.H. Nawar, *J. Alloys Compd.* 611, 50 (2014).
39. M. Amine Fersi, I. Chaabane, and M. Gargouri, *Phys. E* 83, 306 (2016).
40. A. Abkarn, I. Chaabane, and K. Guidara, *Phys. E* 83, 119 (2016).
41. J. Hazarika and A. Kumar, *Phys. B* 481, 268 (2016).
42. N. Moutia, A. Oueslati, M. Ben Gzaiel, and K. Khirouni, *Phys. E* 83, 88 (2016).
43. S. Guidara, H. Feki, and Y. Abid, *J. Alloys Compd.* 663, 424 (2016).
44. A.K. Jonscher, *Universal Relaxation Law* (London: Chelsea Dielectrics Press, 1996).
45. R.H. Chen, R.Y. Chang, and S.C. Shern, *J. Phys. Chem. Solids* 63, 2069 (2002).
46. A.K. Jonscher, *Nature* 267, 673 (1977).
47. S.R. Elliott, *Adv. Phys.* 36, 135 (1987).
48. V.K. Bahatnagar and K.L. Bhatiam, *J. Non Cryst. Solids* 119, 214 (1990).